

# A *GLIMPSE*-based search for 6.7-GHz Methanol Masers and the lifetime of their spectral features

S.P. Ellingsen<sup>1</sup>

<sup>1</sup> *School of Mathematics and Physics, University of Tasmania, Private Bag 21, Hobart, Tasmania 7001, Australia; Simon.Ellingsen@utas.edu.au*

23 May 2018

## ABSTRACT

The University of Tasmania Mt Pleasant 26-m and Ceduna 30-m radio telescopes have been used to search for 6.7-GHz class II methanol masers towards two hundred *GLIMPSE* sources. The target regions were selected on the basis of their mid-infrared colours as being likely to be young high-mass star formation regions and are either bright at 8.0  $\mu\text{m}$ , or have extreme [3.6]-[4.5] colour. Methanol masers were detected towards 38 sites, nine of these being new detections. The prediction was that approximately 20 new 6.7-GHz methanol masers would be detected within 3.5 arcmin of the target *GLIMPSE* sources, but this is the case for only six of the new detections. A number of possible reasons for the discrepancy between the predicted and actual number of new detections have been investigated. It was not possible to draw any firm conclusions as to the cause, but it may be because many of the target sources are at an evolutionary phase prior to that associated with 6.7-GHz methanol masers. Through comparison of the spectra collected as part of this search with those in the literature, the average lifetime of individual 6.7-GHz methanol maser spectral features is estimated to be around 150 years, much longer than is observed for 22-GHz water masers.

**Key words:** masers – stars:formation – ISM: molecules – radio lines : ISM

## 1 INTRODUCTION

In the forty years since their discovery, molecular masers have proven to be powerful signposts of star formation within our Galaxy. The 6.7-GHz  $5_1-6_0$  A<sup>+</sup> transition of methanol is the second strongest of all molecular masers (after the 22-GHz H<sub>2</sub>O transition) and has been shown to trace high-mass star formation regions from a very early evolutionary phase until soon after the formation of an ultra-compact HII region (e.g. Ellingsen 2006; Minier et al. 2005). It also has the advantage that unlike OH and H<sub>2</sub>O masers, 6.7-GHz methanol masers are only associated with high-mass star formation (Minier et al. 2003). To date approximately 520 6.7-GHz methanol masers have been detected (Pestalozzi, Minier & Booth 2005), using three basic strategies; searches targeted towards main-line OH and 12.2-GHz methanol masers (e.g. Menten 1991; MacLeod, Gaylard & Nicolson 1992; MacLeod & Gaylard 1992; Caswell et al. 1995b), searches targeted towards *IRAS* sources with colours characteristic of ultra-compact HII regions (e.g. Schutte et al. 1993; van der Walt, Gaylard & MacLeod 1995; Walsh et al. 1997; Slysh et al. 1999; Szymczak & Kus 2000) and blind searches

of some regions of the Galactic Plane (e.g. Caswell 1996; Ellingsen et al. 1996; Szymczak et al. 2002).

Searches towards sources selected on the basis of their *IRAS*-colours detected many new 6.7-GHz methanol masers, however, they also suffered from a number of shortcomings, in particular false associations and incompleteness. Subsequent observations with better positional accuracy show that in some cases the masers are not associated with the *IRAS* source towards which the search was made (false association). From the point of view of finding new methanol maser sites this is irrelevant, the *IRAS* point source catalogue has led to targeted observations of a high-mass star formation region containing masers. However, it does mean that it is pointless trying to infer much about the physical conditions in the masing region from *IRAS* measurements. This is true even for sources where the masers are associated with the *IRAS* source because the large beamwidth of the *IRAS* observations means that the infrared flux densities measured often include contributions from multiple star formation sites within the larger molecular cloud. The second problem with *IRAS*-based searches is that they fail to detect many maser sites. The untargeted search of Ellingsen et al. (1996) approximately doubled the number

of methanol masers in the regions searched, despite the fact that a number of searches targeted towards OH masers or *IRAS* sources had already been undertaken. Ellingsen et al. (1996) showed that no *IRAS*-based search was able to detect more than 60% of the methanol masers in a given region due to many of the maser sites having no associated *IRAS* source. The absence of an *IRAS* source towards these methanol maser sites is likely due to well-documented problems with confusion and hysteresis in *IRAS* observations of the Galactic Plane and not because there is no far-infrared emission associated with the masers.

In the 20 years since the *IRAS* observations a number of other infrared satellites have made large imaging surveys of the Galactic Plane, in particular *MSX* (Egan et al. 2003) and the *GLIMPSE* survey with the *Spitzer Space Telescope* (Benjamin et al. 2003). The *MSX* observations covered 4 bands from 8 - 21  $\mu\text{m}$  with a resolution of 18 arcsec at 21  $\mu\text{m}$ . The *GLIMPSE* survey was at still shorter wavelengths (4 bands from 3.6 through to 8.0  $\mu\text{m}$ ), but at much higher spatial resolution (1.4–1.9 arcsec). The *MSX* observations are not sufficiently sensitive, nor of high enough angular resolution to provide useful targeting criteria for maser searches (Ellingsen 2005). Previous ground-based mid-infrared observations have found that many methanol maser sources had no associated source at 10  $\mu\text{m}$  (De Buizer et al. 2000; Walsh et al. 2001) and so the prospects for the *GLIMPSE* survey being a useful tool for maser studies might seem poor. However, the higher sensitivity of the space-based observations means that this is not the case and Ellingsen (2006) (hereafter E06) found that more than 90% of 6.7 GHz methanol maser sites are associated with mid-infrared emission visible in the 8.0  $\mu\text{m}$  band. E06 showed that approximately two-thirds of methanol maser sites are associated with a *GLIMPSE* point source and that typically these sources are bright in the 8.0  $\mu\text{m}$  band and have very red mid-infrared colours.

Analysing previous untargeted searches of the Galactic Plane, E06 found that approximately 10% of *GLIMPSE* point sources which have 8.0- $\mu\text{m}$  intensity less than tenth magnitude ( $[8.0] < 10$ ) and colour between the 3.6- and 4.5- $\mu\text{m}$  bands greater than 1.3 magnitudes ( $[3.6]-[4.5] > 1.3$ ) were associated with methanol masers. They also found that such a search of all sources meeting these *GLIMPSE*-based criteria within a given region would detect more than 80% of all the methanol masers in the region (some of these would be serendipitous detections where the maser is not associated with a targeted *GLIMPSE* source, but merely nearby). The *GLIMPSE* point source catalogue contains more than 30 million sources and of these 5675 meet the criteria outlined by E06. Statistically, these cannot all be young high-mass star forming regions, and there must be contamination of the sample by other objects (E06 suggested low-mass class 0 objects as one example). Clearly it is desirable to determine if it is possible to further refine the sample to increase the percentage of targeted sources that have an associated 6.7-GHz methanol maser. Many of the *GLIMPSE* point sources that meet the criteria lie very close to one or another of the cut-offs and it may well be that the percentage of contaminating sources increases closer to the criterion limits. To test this hypothesis I selected the 100 most extreme sources meeting each criterion and searched for 6.7-GHz methanol maser emission towards these sources.

Despite excluding *GLIMPSE* sources close to known 6.7-GHz methanol masers from the target sample (see section 2), the redetection of some previously detected masers is inevitable in any large search. The majority of the currently known 6.7-GHz methanol masers were discovered more than a decade ago and so comparison of a current epoch spectrum with those in the literature provides an opportunity to assess the long-term variability of 6.7-GHz methanol masers. The variability of a large sample of 6.7-GHz methanol masers on timescales of a few months to a year was investigated by Caswell et al. (1995a). They found the variability on a timescale of a year is typically less than a factor of two, but sometimes is more extreme. They also found greater variability was more prevalent in masers with weaker peak flux density. Goedhart et al. (2004) observed a sample of 54 sources regularly for more than four years and observed a range of different types of variability, including periodic variations which are not observed in water or OH masers in star formation regions. These observations showed significant variability in more than half of the spectral features analysed, suggesting the sparse sampling of Caswell et al. (1995a) underestimated the true variability.

22-GHz water masers are known to exhibit much more extreme variability than is observed in 6.7-GHz methanol masers, with many individual spectral features having lifetimes of around one year (Brand et al. 2003). Goedhart et al. (2004) found only one of 54 6.7-GHz methanol masers (Mon R2) showed significant changes in its spectral profile, similar to the variations commonly observed in water masers. van der Walt (2005) estimates the lifetime of 6.7-GHz methanol maser sources to be in the range  $2.5\text{--}4.5 \times 10^4$  years. Individual spectral features might be expected to have significantly shorter lifetimes, and by comparing how many spectral features have disappeared and appeared over a ten year period for a sample of sources it should be possible to estimate the average lifetime of typical 6.7-GHz methanol maser spectral features/spots.

## 2 OBSERVATIONS AND DATA REDUCTION

To test the predictions of E06 I have carried out a search for 6.7-GHz methanol masers towards 200 *GLIMPSE* point sources. To do this I started with the sample of 5675 *GLIMPSE* point sources that meet both criteria  $[8.0] < 10$  and  $[3.6]-[4.5] > 1.3$ . The sample was drawn from the 2005 April 15 release of the *GLIMPSE* point source catalogue and point sources without measurements in all three of these bands were excluded. From this sample of 5675 sources I removed those that lay within 3.5 arcmin of a methanol maser source listed in the Pestalozzi et al. (2005) catalogue (3.5 arcmin is half the FWHM of the Mt Pleasant radio telescope at 6.7 GHz). This left a total of 4878 *GLIMPSE* point sources and from these I extracted the 100 sources strongest in the 8.0- $\mu\text{m}$  band and the 100 sources with the largest  $[3.6]-[4.5]$  colour. The hundred sources selected on the basis of their 8.0- $\mu\text{m}$  strength have an intensity of 4.58 magnitudes or less (hereafter referred to as category B sources) and the 100 reddest sources have  $[3.6]-[4.5]$  colour greater than 2.87 magnitudes (category A). Figure 1 shows a colour-magnitude diagram of the selected sources, compared to all sources within a 30-arcsecond radius of  $\ell = 326.5^\circ$ ,  $b = 0.0^\circ$ . This shows

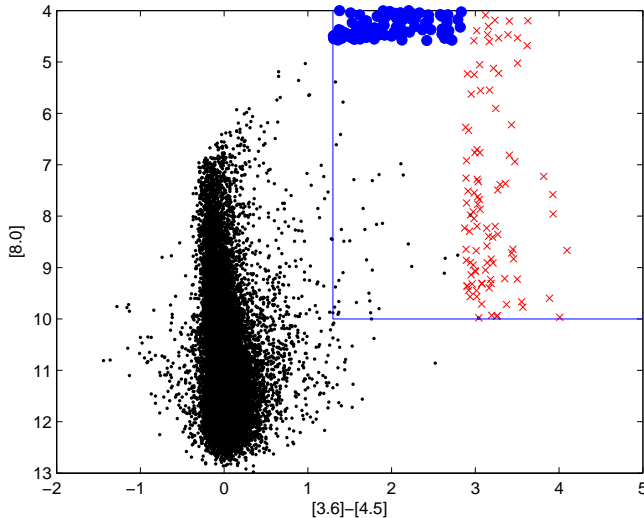


**Figure 1.** A [3.6]-[4.5] versus [8.0] colour-magnitude diagram for the *GLIMPSE* point sources searched for 6.7-GHz methanol masers. The crosses are the sources with red [3.6]-[4.5] colour (category A), the circles are the sources with intense 8.0- $\mu\text{m}$  emission (category B) and the dots are the *GLIMPSE* point sources within 30 arcsec of  $\ell=326.5^\circ$ ,  $b = 0.0^\circ$  which have measurements in all of the 3.6-, 4.5- and 8.0- $\mu\text{m}$  bands (21992 of 109053 sources). The box marks the borders of the region identified by E06 as containing sources likely to be young high-mass star forming regions.

that the selected sources have very different properties to the majority of *GLIMPSE* sources.

The observations were made between 2005 July-December using the University of Tasmania Mt Pleasant 26m and Ceduna 30m radio telescopes. A rest frequency of 6.668518 GHz for the  $5_1-6_0$  A<sup>+</sup> transition was used in the observations and data processing. A more precise determination of the rest frequency determined by Breckenridge & Kukolich (1995) measured it to be 6.6685192(8) GHz, and the frequency difference of 1.2 kHz corresponds to a velocity change of 0.05 km s<sup>-1</sup>. As this is less than the accuracy to which the peak velocity can easily be determined, no correction has been made to the velocity scale to account for this. At 6.7 GHz the half-power beam width of the Mt Pleasant and Ceduna antennas are 7 and 6 arcmin respectively. The majority of the initial search observations were made at Mt Pleasant, as were all the final spectra (except G345.20-0.04). Ceduna was used for some repeat observations (where the initial observations were affected by internally generated interference) and to determine better positions for some sources. The Mt Pleasant observations were made using a cryogenically cooled receiver with dual orthogonal circular polarizations each with a system temperature which varied between 750-1400 Jy depending on the day. The data were collected using a 2-bit digital autocorrelation spectrometer configured with 4096 channels spanning a 4-MHz bandwidth. For an observing frequency of 6.7 GHz this configuration yields a natural weighting (i.e. no Hanning or other smoothing) velocity resolution of 0.044 km s<sup>-1</sup>. The Ceduna observations were made with an uncooled receiver with dual orthogonal circular polarizations each with a system temperature of approximately 500 Jy.

The Ceduna correlator was identical to that used at Hobart, however due to technical problems only 2048 channels were available meaning that the natural weighting velocity resolution was 0.105 km s<sup>-1</sup>.

Each *GLIMPSE* source was observed for 10 minutes on-source, using an observation of a nearby target for the off-source reference. This yielded a typical RMS between 0.5 and 0.6 Jy after the spectrum had been smoothed with 5-point box car (giving an effective velocity resolution of 0.22 km s<sup>-1</sup>). Some class II methanol masers exhibit very narrow spectral features with Szymczak & Kus (2000) showing the median velocity full-width half maximum of the methanol masers they observed to be 0.14 km s<sup>-1</sup>. To avoid missing weaker masers with very narrow features spectra were also produced for each source with only Hanning smoothing applied. This yields a velocity resolution of 0.088 km s<sup>-1</sup> and a typical RMS between 0.8 and 0.9 Jy. For each of the spectra showing likely maser emission, a 5-point grid observation (with observations made at 4 points forming a square, each offset from the fifth, central position by 3.5 arcminutes) was made to better determine the maser position. A non-linear least squares fit of a 2-dimensional Gaussian with the same dimensions as the telescope beam was made to the data from the grid observations in order to better determine the location of the maser emission. In a few cases the masers were significantly offset from the targeted *GLIMPSE* source and the process had to be repeated to refine the position. Once an accurate position had been determined a final, sensitive observation of all the detected sources was then made. A 5-point grid observation was also made at the same time as the final spectrum and the measured positional offset used to correct the flux density scale for primary beam attenuation (typically this correction was less than 10 per cent). Through comparison of the measured and known positions for sources that have been previously detected the pointing accuracy of the system is estimated to be approximately 0.5 arcmin.

### 3 RESULTS

A search of 200 *GLIMPSE* sources has resulted in the detection of thirty eight 6.7-GHz methanol masers, nine of these being new discoveries (see Table 1). Methanol maser emission was detected in the spectra of 27 *GLIMPSE* sources, with nine of these containing two separate sites and one three, leading to a total of 38 detections. Table 1 lists the 6.7-GHz methanol maser sources detected, their location and the *GLIMPSE* source they were detected towards. Sources with no entry in the *GLIMPSE* column were typically detected when making grid or final observations of the previous source in the table. Table 2 summarises the characteristics of the maser emission, including the peak flux density, velocity range and integrated flux density of the sources.

An oversight during the formulation of the sample meant that there were two cases where two *GLIMPSE* sources with only a small separation between them were observed (these being GLMC G 321.9359–0.0061 & GLMC G 321.9367–0.0063 and GLMC G 345.2563–0.0366 & GLMC G 345.2574–0.0351 ). So effectively a total of 198 locations were searched for 6.7-GHz methanol masers in this work. Table 3 lists the *GLIMPSE* point sources observed

**Table 1.** 6.7-GHz methanol maser sources detected towards *GLIMPSE* sources. Sources marked with a \* are new detections. See the catalogue of Pestalozzi et al. (2005) for the references for previously detected sources. Those listed as being in category A were selected on the basis of having a large [3.6]-[4.5] excess, while those in category B were selected on the basis of high intensity in the 8.0  $\mu\text{m}$  band.

Methanol maser name	Right Ascension (J2000)	Declination (J2000)	<i>GLIMPSE</i> PSC name	Category	Angular Separation (arcmin)
G 305.21+0.21	13:11:14.4	-62:34:26	GLMC G 305.4450+0.2644	A	14.5
G 305.20+0.21	13:11:10.6	-62:34:39			
G 316.81-0.06	14:45:26.4	-59:49:17	GLMC G 316.7626-0.0128	A	4.0
G 317.47-0.41*	14:51:22.5	-59:51:07	GLMC G 317.4656-0.4026	A	0.5
G 320.23-0.29	15:09:52.0	-58:25:38	GLMC G 320.3686-0.2804	A	8.2
G 323.46-0.08	15:29:19.3	-56:31:23	GLMC G 323.4702-0.1421	B	3.9
G 323.74-0.26	15:31:45.4	-56:30:50	GLMC G 323.5478+0.0237	A	20.7
G 326.66+0.52	15:45:02.9	-54:09:03	GLMC G 326.7077+0.5828	A	4.6
G 326.64+0.61	15:44:33.2	-54:05:31			
G 328.24-0.55	15:57:58.3	-53:59:23	GLMC G 328.2558-0.4124	A	8.2
G 328.25-0.53	15:57:59.9	-53:58:01			
G 331.56-0.12	16:12:27.2	-51:27:37	GLMC G 331.6047-0.0724	B	4.1
G 331.54-0.07	16:12:08.8	-51:25:47			
G 337.15-0.04*	16:37:50.9	-47:39:09	GLMC G 337.1393-0.3803	A	1.6
G 337.39-0.20*	16:37:55.9	-47:20:58	GLMC G 337.3444-0.1807	A	3.2
G 339.88-1.26	16:52:04.7	-46:08:34	GLMC G 339.8712-0.6697	B	35.4
G 340.97-1.03*	16:54:58.7	-45:09:23	GLMC G 340.9108-1.0316	A	3.5
G 343.52-0.50*	17:01:27.7	-42:49:44	GLMC G 343.5015-0.4724	A	1.7
G 345.20-0.04*	17:05:01.0	-41:13:09	GLMC G 345.2563-0.0366	A	3.6
G 11.15-0.14*	18:10:28.1	-19:22:40	GLMC G 011.2013-0.1570	A	6.2
G 18.99-0.04*	18:25:44.1	-12:24:15	GLMC G 019.0087-0.0293	A	1.5
G 23.01-0.41	18:34:40.2	-09:00:36	GLMC G 022.9600-0.4752	B	4.9
G 24.14+0.00	18:35:20.8	-07:48:48	GLMC G 024.2356-0.0570	B	5.6
G 25.82-0.17	18:39:03.6	-06:24:10	GLMC G 025.8062-0.2845	B	6.5
G 27.28+0.15	18:40:34.5	-04:57:14	GLMC G 027.2788+0.2095	B	3.6
G 27.21+0.26	18:40:03.8	-04:58:09			
G 28.02-0.44	18:44:02.1	-04:34:14	GLMC G 027.9676-0.4747	A	3.8
G 29.86-0.04	18:45:59.5	-02:44:47	GLMC G 029.8400-0.0973	B	3.7
G 29.95-0.02	18:46:03.7	-02:39:21			
G 30.20-0.17	18:47:03.5	-02:30:31			
G 30.70-0.07	18:47:36.9	-02:01:05	GLMC G 030.6721+0.0141	A	5.3
G 30.76-0.05	18:47:39.7	-01:57:22			
G 30.79+0.20	18:46:48.1	-01:48:46	GLMC G 030.8070+0.0803	B	7.5
G 30.78+0.23	18:46:41.5	-01:48:32			
G 30.82-0.05	18:46:37.4	-01:45:14			
G 31.04+0.36	18:46:41.5	-01:30:42	GLMC G 031.0431+0.2820	A	5.1
G 35.20-0.74	18:58:12.7	+01:40:50	GLMC G 035.1293-0.7427	A	4.2
G 35.18-0.74*	18:58:09.8	+01:39:36			

which contained no detected 6.7-GHz methanol maser emission. For each source it gives the velocity range covered by the spectrum and the RMS in the smoothed (velocity resolution 0.22 km s<sup>-1</sup>) spectrum.

Figure 2 shows Hanning smoothed spectra (velocity resolution 0.088 km/s) of each of the detected 6.7-GHz methanol masers made with the Hobart radio telescope. In many cases the only spectra available in the literature for the previously detected sources were observed more than a decade ago (Caswell et al. 1995b; Walsh et al. 1997) and so the spectra of all detected sources are shown here to enable variability comparisons to be made. The sources which show significant variability are noted in section 3.1.

The last column in Table 1 shows the separation between the methanol maser and the *GLIMPSE* source. As expected from the process used to select the target *GLIMPSE* sources, all the previously known methanol masers are sep-

arated from them by more than 3.5 arcmin. In general the newly discovered sources are within a few arcminutes of the *GLIMPSE* source, although in most cases the separation is significantly greater than the pointing accuracy (0.5 arcmin), so it is unlikely that the masers and infrared sources are directly associated.

### 3.1 Comments on individual sources

*G305.20+0.21/G305.21+0.21/G305.25+0.25:*

G305.20+0.21 and G305.21+0.21 are separated by 22 arcsec and hence cannot be readily distinguished by these observations. Walsh & Burton (2006) suggest that this pair of sources consists of two star formation regions in different evolutionary stages, G305.21+0.21 being younger and G305.20+0.21 more evolved. G305.21+0.21 has a very similar peak intensity and spectral morphology to that

**Table 2.** Properties of the 6.7-GHz methanol maser sources detected.

Methanol maser name	Peak Flux Density (Jy)	Peak Vel. (km s <sup>-1</sup> )	Velocity range (km s <sup>-1</sup> )	Integrated Flux Density (Jykm s <sup>-1</sup> )
G 305.21+0.21	488	-38.5	-39.8 – -34.6	377.8
G 316.81–0.06	71	-45.8	-47.2 – -42.0	74.1
G 317.47–0.41	61	-37.7	-42.2 – -36.9	109.1
G 320.23–0.29	30	-62.2	-71.1 – -59.0	45.8
G 323.46–0.08	18	-67.0	-67.3 – -66.6	9.7
G 323.74–0.26	3450	-50.6	-57.2 – -42.8	5556.9
G 326.66+0.52	15	-37.3	-41.4 – -36.2	10.5
G 328.24–0.55	955	-44.8	-46.3 – -33.6	560.2
G 331.56–0.12	61	-97.2	-104.9 – -94.3	73.2
G 337.15–0.40	24	-49.4	-49.8 – -48.2	19.8
G 337.39–0.20	36	-56.4	-65.8 – -52.1	51.3
G 339.88–1.26	1629	-38.8	-39.9 – -31.8	2898.6
G 340.97–1.03	10	-31.4	-32.2 – -20.1	3.7
G 343.52–0.50	4	-39.0	-42.3 – -38.0	2.9
G 345.20–0.04	3	-0.7	-1.0 – 0.0	2.1
G 11.15–0.14	26	32.3	18.6 – 33.7	33.4
G 18.99–0.04	20	55.4	54.5 – 60.1	20.0
G 23.01–0.41	442	74.8	72.3 – 83.2	806.3
G 24.14+0.00	30	17.4	17.1 – 18.0	20.6
G 25.82–0.17	78	91.6	90.0 – 99.4	89.2
G 27.28+0.15	36	34.8	34.3 – 35.5	18.9
G 27.21+0.26	7	9.1	7.6 – 9.8	5.5
G 28.02–0.44	4	16.8	16.0 – 28.0	3.5
G 29.86–0.04	81	101.4	99.9 – 104.3	112.8
G 30.20–0.17	22	108.5	104.5 – 110.9	26.4
G 30.70–0.07	154	88.2	85.7 – 90.0	85.8
G 30.79+0.20	19	87.4	76.1 – 102.0	51.2
G 30.82–0.05	13	91.7	90.7 – 109.3	28.3
G 31.04+0.36	4	80.7	79.2 – 81.4	3.3
G 35.18–0.74	44	36.7	29.5 – 37.8	49.5
G 35.20–0.74	148	28.5	27.0 – 35.0	136.8

seen more than a decade ago by Caswell et al. (1995b) and Goedhart, Gaylard & van der Walt (2004) observed this source to show relatively little variability. G305.20+0.21 shows a modest increase in intensity, also consistent with the observations of Goedhart et al. (2004)

Emission from G305.25+0.25 was also detected in this observation covering a velocity range from -33 – -28 km s<sup>-1</sup>, but is too weak to be easily seen on the scale shown in Fig. 2. These observations show the source to have peaks near -29 and -32 km s<sup>-1</sup>, each of about 6 Jy, significantly stronger than the only previous observation of G305.25+0.25 by Caswell et al. (1995b) in September 1992, who observed it to have a peak flux density of about 2 Jy.

*G316.81-0.06:* This source has been observed on numerous previous occasions; the observations of MacLeod & Gaylard (1992) measured the flux density of the emission at -46 km s<sup>-1</sup> to be about 10 Jy in late 1991. The observations of Caswell, Vaile & Ellingsen (1995a) in 1992/3 exhibit significant changes in the relative flux density of the different spectral features, and they list it as showing significant variability. Figure 2 shows that two strongest spectral components in this source have increased in flux density by more than a factor of four since 1992, while some of the weaker features have dropped below the detection limit of the current observations.

*G317.47-0.41:* This is the strongest of the newly de-

tected 6.7-GHz methanol masers with a peak flux density of approximately 60 Jy and three strong peaks over a velocity range of 6 km s<sup>-1</sup>.

*G320.23-0.29:* Although this source is listed as being variable by Caswell et al. (1995a) the velocity range, peak flux density and general appearance are very similar to those observed more than a decade ago (MacLeod & Gaylard 1992; Caswell et al. 1995b; Walsh et al. 1997). The only exception is that a spectral feature present near -69.5 km s<sup>-1</sup> with a peak flux density of about 4 Jy is not present in the current observations.

*G323.74-0.26:* This is one of the strongest 6.7-GHz methanol masers and has been the subject of detailed study by Walsh et al. (2002). Its intensity is also the reason that it was found by this survey, as it was detected in observations of a *GLIMPSE* source more than 20 arcmin from the maser site. It is listed as not variable by Caswell et al. (1995b), but Goedhart et al. (2004) observed the source to exhibit moderate variations, some highly correlated between spectral features. A comparison of the spectrum in Fig. 2 with that of Caswell et al. (1995b) shows an increase of the order of 10 per cent in the peak flux density and changes in the relative intensity of most features. The 6.7-GHz methanol maser emission in this source was observed in late 2003 (two years prior to the current observations) by Ellingsen et al. (2004) and that spectrum is shown using a dashed line in

**Table 3.** *GLIMPSE* sources searched for 6.7-GHz methanol maser emission for which there was no detection. Those listed as being in category A were selected on the basis of having a large [3.6]-[4.5] excess, while those in category B were selected on the basis of high intensity in the 8.0  $\mu\text{m}$  band. The RMS quoted is for the spectrum after box car smoothing to a velocity resolution of 0.22 km s<sup>-1</sup>.

<i>GLIMPSE</i> PSC name	Category	Right Ascension (J2000)	Declination (J2000)	RMS (Jy)	Velocity Range (km s <sup>-1</sup> )
GLMC G 301.1149+0.0094	A	12:35:31.4	-62:48:22	0.5	-134 – 45
GLMC G 301.3438+0.0134	A	12:37:31.5	-62:48:55	0.5	-134 – 45
GLMC G 302.4547–0.7406	B	12:47:08.6	-63:36:30	0.5	-133 – 46
GLMC G 302.6482+0.9860	B	12:49:01.7	-61:53:04	0.5	-134 – 45
GLMC G 304.0642+0.4367	A	13:01:13.2	-62:24:49	0.5	-133 – 46
GLMC G 304.6740+0.2569	A	13:06:34.1	-62:33:49	0.5	-133 – 46
GLMC G 305.1384–0.3755	B	13:11:00.3	-63:09:48	0.5	-132 – 47
GLMC G 306.0949–0.4782	B	13:19:31.8	-63:10:38	0.5	-132 – 47
GLMC G 307.8055–0.4560	A	13:34:27.5	-62:55:12	0.5	-131 – 48
GLMC G 308.1289–0.2989	A	13:37:00.8	-62:42:35	0.5	-131 – 48
GLMC G 309.0355–0.2859	B	13:44:43.9	-62:31:28	0.6	-131 – 48
GLMC G 309.1685–0.5511	A	13:46:20.7	-62:45:22	0.6	-131 – 48
GLMC G 310.1545+0.3379	B	13:52:53.2	-61:40:09	0.6	-131 – 48
GLMC G 310.3102+0.6306	A	13:53:34.3	-61:20:52	0.6	-131 – 48
GLMC G 310.5706–0.1905	A	13:57:24.3	-62:04:48	0.6	-131 – 48
GLMC G 310.6793+0.4858	A	13:56:51.4	-61:23:53	0.6	-132 – 47
GLMC G 311.2947–0.3779	B	14:03:47.6	-62:04:09	0.6	-132 – 32
GLMC G 311.4166+0.9159	A	14:01:49.3	-60:47:28	0.6	-132 – 32
GLMC G 312.3296–0.0874	A	14:11:27.4	-61:29:26	0.6	-132 – 47
GLMC G 312.4354–0.7425	B	14:14:01.3	-62:04:51	0.6	-131 – 47
GLMC G 312.7411+0.0787	A	14:14:17.5	-61:12:18	0.5	-132 – 32
GLMC G 314.4714–1.0256	B	14:31:03.7	-61:38:42	0.5	-131 – 32
GLMC G 315.0424+0.1836	A	14:31:40.6	-60:18:35	0.5	-131 – 32
GLMC G 315.3154+0.9171	B	14:31:29.4	-59:31:39	0.5	-131 – 32
GLMC G 317.4663–0.0668	A	14:50:09.2	-59:32:46	0.5	-130 – 35
GLMC G 317.8897–0.2531	A	14:53:47.9	-59:31:25	0.6	-128 – 51
GLMC G 318.7221–0.3129	A	14:59:48.4	-59:11:28	0.6	-127 – 52
GLMC G 319.3711–0.7818	B	15:06:01.4	-59:17:18	0.5	-127 – 52
GLMC G 321.9359–0.0061	A	15:19:43.0	-57:18:07	0.5	-128 – 51
GLMC G 321.9367–0.0063	A	15:19:43.3	-57:18:06	0.5	-128 – 51
GLMC G 324.8889–0.4130	B	15:39:06.1	-55:57:55	0.6	-125 – 54
GLMC G 326.7527+0.7101	A	15:44:44.8	-53:56:44	0.6	-124 – 55
GLMC G 326.9249–0.5142	A	15:50:52.9	-54:48:01	0.6	-124 – 55
GLMC G 326.9646–0.0130	A	15:48:56.0	-54:23:04	0.5	-107 – 72
GLMC G 326.9872–0.0306	A	15:49:07.8	-54:23:02	0.7	-120 – 50
GLMC G 327.4618–0.1516	B	15:52:11.0	-54:10:50	0.7	-120 – 55
GLMC G 328.0585+0.3694	A	15:53:04.8	-53:23:59	0.6	-125 – 54
GLMC G 328.2162–0.0216	A	15:55:34.4	-53:36:02	0.6	-126 – 40
GLMC G 328.9849–0.4363	B	16:01:19.1	-53:25:05	0.6	-125 – 54
GLMC G 329.1065–0.0699	B	16:00:19.8	-53:03:41	0.6	-125 – 54
GLMC G 329.4935+0.1053	A	16:01:30.5	-52:40:32	0.5	-125 – 54
GLMC G 329.6382–1.0601	B	16:07:22.8	-53:27:03	0.5	-125 – 54
GLMC G 329.7182+0.8046	A	15:59:37.6	-51:59:58	0.5	-125 – 40
GLMC G 331.3051–0.4970	B	16:12:56.1	-51:54:22	0.7	-80 – 65
GLMC G 331.6119–0.2711	A	16:13:22.5	-51:31:52	0.8	-107 – 72
GLMC G 331.7238–0.2039	A	16:13:36.1	-51:24:20	0.8	-107 – 72
GLMC G 332.1934+0.1313	A	16:14:18.2	-50:50:21	0.3	-149 – 30
GLMC G 334.4183+0.0581	A	16:24:30.8	-49:19:52	0.5	-123 – 42
GLMC G 334.5468+0.4889	A	16:23:11.4	-48:56:13	0.5	-123 – 42
GLMC G 336.0800+0.4807	B	16:29:39.4	-47:50:32	0.2	-148 – 31
GLMC G 336.2340+0.5070	B	16:30:10.4	-47:42:45	0.3	-148 – 31
GLMC G 338.3874+0.7252	B	16:37:46.8	-45:58:56	0.7	-119 – 60
GLMC G 339.5350–0.0524	B	16:45:28.7	-45:38:02	0.6	-121 – 48
GLMC G 340.0314+0.6002	B	16:49:25.3	-45:46:35	0.7	-120 – 59
GLMC G 340.4215–0.0222	B	16:44:30.5	-44:49:55	0.3	-148 – 31
GLMC G 340.8223–1.0286	B	16:48:36.7	-44:56:19	0.6	-119 – 60
GLMC G 340.9942–0.3102	A	16:54:27.3	-45:16:14	0.6	-119 – 60
GLMC G 341.0242+0.1975	B	16:51:55.5	-44:40:59	0.5	-119 – 47

Table 3 – *continued*

<i>GLIMPSE</i> PSC name	Category	Right Ascension (J2000)	Declination (J2000)	RMS (Jy)	Velocity Range (km s <sup>-1</sup> )
GLMC G 342.3190+0.5876	A	16:49:50.5	-44:20:08	0.7	-117 – 62
GLMC G 342.5437-0.7020	B	16:52:44.7	-43:05:22	0.6	-117 – 62
GLMC G 342.7816+0.1588	A	16:59:03.2	-43:43:21	0.6	-116 – 63
GLMC G 342.8209+0.3827	A	16:56:09.8	-43:00:01	0.6	-119 – 60
GLMC G 343.7378-0.1116	A	16:55:20.7	-42:49:46	0.5	-118 – 61
GLMC G 344.1581-0.0748	A	17:00:33.0	-42:25:07	0.6	-118 – 47
GLMC G 344.2931-0.7158	A	17:01:47.3	-42:03:52	0.6	-118 – 47
GLMC G 345.2574-0.0351	A	17:04:58.6	-42:20:53	0.3	-149 – 30
GLMC G 345.6528-1.0043	B	17:10:35.7	-41:25:57	0.7	-115 – 64
GLMC G 345.7172+0.8166	B	17:03:06.4	-40:17:09	0.4	-145 – 34
GLMC G 345.8590-0.6792	B	17:09:51.3	-41:04:25	0.3	-149 – 30
GLMC G 346.1045-0.4612	B	17:09:42.0	-40:44:47	0.3	-148 – 30
GLMC G 347.2918+0.1330	A	17:10:53.1	-39:26:18	0.4	-145 – 34
GLMC G 347.4007+0.1229	A	17:11:15.7	-39:21:24	0.4	-145 – 34
GLMC G 347.7014+0.9183	B	17:08:53.2	-38:38:32	0.4	-144 – 34
GLMC G 348.5661+0.1626	A	17:14:36.9	-38:23:25	0.5	-113 – 66
GLMC G 348.9414-0.1082	B	17:16:51.1	-38:14:33	0.6	-112 – 67
GLMC G 349.1465-0.9766	B	17:21:04.9	-38:34:25	0.5	-112 – 67
GLMC G 349.2867+0.4602	A	17:15:31.2	-37:37:53	0.5	-112 – 67
GLMC G 349.3072+0.3703	B	17:15:57.0	-37:40:01	0.5	-112 – 67
GLMC G 349.5204-0.2641	B	17:19:11.6	-37:51:34	0.5	-112 – 67
GLMC G 349.8799+0.5500	A	17:16:53.1	-37:05:47	0.6	-112 – 67
GLMC G 011.1080+0.2045	B	18:09:17.1	-19:13:19	0.6	-56 – 123
GLMC G 011.1158+0.0513	B	18:09:52.2	-19:17:21	0.6	-56 – 123
GLMC G 011.2354-0.9595	B	18:13:52.4	-19:40:14	0.6	-56 – 123
GLMC G 011.3446+0.7971	A	18:07:34.8	-18:43:39	0.6	-56 – 123
GLMC G 011.3802-0.0068	B	18:10:37.5	-19:05:09	0.5	-56 – 123
GLMC G 012.2200-0.3339	A	18:13:32.6	-18:30:24	0.6	-56 – 123
GLMC G 012.5764+0.3089	B	18:11:53.3	-17:53:08	0.2	-58 – 121
GLMC G 012.6896+0.2881	B	18:12:11.7	-17:47:46	0.5	-56 – 123
GLMC G 013.2348-0.0723	A	18:14:37.1	-17:29:25	0.2	-58 – 120
GLMC G 013.2690-0.3487	A	18:15:42.4	-17:35:32	0.7	-59 – 119
GLMC G 013.2853+0.5723	B	18:12:21.0	-17:08:14	0.5	-56 – 123
GLMC G 013.2894+0.2129	B	18:13:40.7	-17:18:21	0.5	-56 – 123
GLMC G 014.1087-0.5688	A	18:18:11.3	-16:57:28	0.5	-55 – 124
GLMC G 014.1520-0.5173	B	18:18:05.1	-16:53:43	0.6	-55 – 124
GLMC G 014.4758-0.1259	A	18:17:17.2	-16:25:28	0.6	-55 – 124
GLMC G 014.6786+0.0394	A	18:17:04.9	-16:10:03	0.2	-58 – 120
GLMC G 014.7210+0.1682	B	18:16:41.6	-16:04:09	0.3	-58 – 120
GLMC G 014.8008-0.1372	A	18:17:58.3	-16:08:38	0.3	-59 – 120
GLMC G 015.0296+0.8534	A	18:14:48.1	-15:28:17	0.3	-59 – 120
GLMC G 015.0918-0.2690	A	18:19:01.7	-15:57:00	0.6	-51 – 120
GLMC G 015.2571-0.1561	A	18:18:56.3	-15:45:03	0.6	-57 – 121
GLMC G 015.5709-0.7953	B	18:21:53.8	-15:46:32	0.6	-57 – 122
GLMC G 016.0634-0.9387	B	18:23:22.9	-15:24:29	0.5	-57 – 122
GLMC G 016.4464-0.3874	A	18:22:06.6	-14:48:40	0.5	-57 – 122
GLMC G 016.6638+0.6325	B	18:18:49.1	-14:08:18	0.5	-57 – 122
GLMC G 016.6786+0.1714	B	18:20:31.4	-14:20:35	0.7	-55 – 124
GLMC G 016.8016-0.2707	A	18:22:22.4	-14:26:33	0.7	-55 – 124
GLMC G 016.8056+0.8149	B	18:18:25.9	-13:55:38	0.7	-55 – 124
GLMC G 016.9750-0.0291	A	18:21:49.8	-14:10:34	0.7	-55 – 124
GLMC G 017.1767-0.8367	B	18:25:09.9	-14:22:35	0.3	-59 – 119
GLMC G 017.5043-0.6885	B	18:25:15.3	-14:01:03	0.6	-54 – 125
GLMC G 018.0544+0.9845	B	18:20:14.5	-12:44:47	0.6	-54 – 125
GLMC G 018.4478-0.3116	B	18:25:41.8	-13:00:26	0.7	-54 – 125
GLMC G 019.0529+0.6390	B	18:23:24.8	-12:01:40	0.7	-54 – 125
GLMC G 019.7592+0.1095	A	18:26:40.5	-11:39:02	0.6	-56 – 123
GLMC G 019.8905+0.2470	B	18:26:25.7	-11:28:14	0.6	-56 – 123
GLMC G 019.9230-0.2581	B	18:28:18.9	-11:40:37	0.6	-55 – 124
GLMC G 020.5655+0.9478	B	18:25:11.1	-10:32:48	0.6	-55 – 123

Table 3 – *continued*

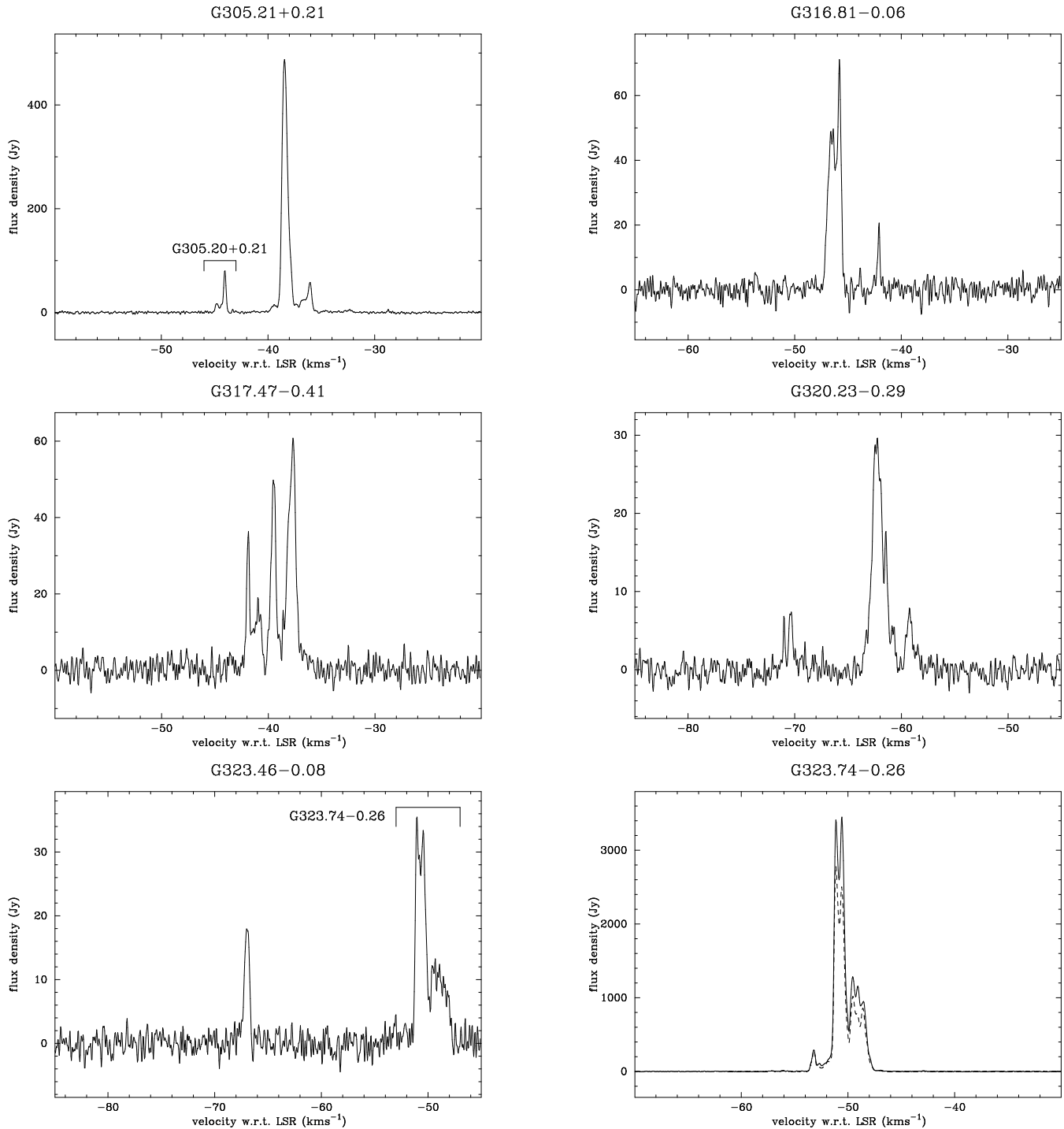
<i>GLIMPSE</i> PSC name	Category	Right Ascension (J2000)	Declination (J2000)	RMS (Jy)	Velocity Range (km s <sup>-1</sup> )
GLMC G 020.8544+0.4858	B	18:27:23.8	-10:30:23	0.5	-55 – 124
GLMC G 021.5349+1.0505	A	18:26:39.2	-09:38:28	0.6	-55 – 124
GLMC G 022.1572-0.5487	A	18:33:34.5	-09:49:51	0.8	-52 – 127
GLMC G 022.2912+0.8678	B	18:28:44.0	-09:03:24	0.7	-53 – 126
GLMC G 022.4514-0.4332	B	18:33:42.5	-09:31:00	0.7	-52 – 127
GLMC G 022.9242+0.2235	B	18:32:14.0	-08:47:39	0.7	-52 – 127
GLMC G 023.4058+0.4485	A	18:32:19.5	-08:15:47	0.7	-52 – 127
GLMC G 023.4310-0.5183	A	18:35:50.5	-08:41:11	0.8	-51 – 128
GLMC G 023.6155-0.0071	A	18:34:21.0	-08:17:14	0.8	-51 – 128
GLMC G 024.3718+0.2933	A	18:34:40.8	-07:28:39	0.7	-52 – 127
GLMC G 024.6333+0.1532	A	18:35:40.1	-07:18:35	0.6	-53 – 126
GLMC G 025.9114-1.0679	B	18:42:24.2	-06:44:02	0.6	-53 – 126
GLMC G 026.4958+0.7106	B	18:37:07.3	-05:23:58	0.6	-53 – 126
GLMC G 026.5027-0.5410	B	18:41:36.3	-05:58:02	0.5	-52 – 126
GLMC G 027.1474-0.1431	A	18:41:22.1	-05:12:43	0.6	-50 – 129
GLMC G 027.6673-0.0548	B	18:42:00.5	-04:42:33	0.7	-50 – 129
GLMC G 028.0827-0.7427	B	18:45:13.6	-04:39:14	0.7	-50 – 129
GLMC G 028.8128+0.2641	A	18:42:58.3	-03:32:41	0.6	-52 – 127
GLMC G 029.3077+0.3218	A	18:43:40.4	-03:04:41	0.6	-52 – 127
GLMC G 030.1029-0.0789	A	18:46:33.3	-02:33:13	0.7	-49 – 130
GLMC G 030.3943-0.7064	B	18:49:19.4	-02:34:50	0.7	-48 – 130
GLMC G 030.4003-1.0657	B	18:50:36.9	-02:44:20	0.7	-48 – 131
GLMC G 030.6039+0.1760	A	18:46:33.7	-01:59:29	0.7	-49 – 130
GLMC G 030.6670-0.3319	B	18:48:29.2	-02:10:01	0.7	-49 – 130
GLMC G 030.6874+0.3592	B	18:46:03.7	-01:50:01	0.6	-51 – 128
GLMC G 031.6615+0.3668	B	18:47:48.8	00:57:48	0.6	-48 – 131
GLMC G 033.5681-0.3841	B	18:53:57.9	00:23:28	0.6	-48 – 131
GLMC G 034.4049+0.0316	B	18:54:00.7	01:19:31	0.7	-48 – 131
GLMC G 034.6817+0.8551	A	18:51:35.0	01:56:50	0.6	-50 – 129
GLMC G 036.1695+0.2392	B	18:56:29.7	02:59:25	0.6	-49 – 130
GLMC G 037.2004-0.0019	B	18:59:14.4	03:47:50	0.6	-48 – 131
GLMC G 038.9985-0.5075	A	19:04:20.8	05:09:52	0.7	-45 – 134
GLMC G 040.1332+0.9389	B	19:01:16.0	06:50:08	0.6	-45 – 134
GLMC G 040.1647+0.2958	B	19:03:37.6	06:34:09	0.6	-45 – 134
GLMC G 041.2075-0.0235	B	19:06:41.9	07:20:57	0.7	-45 – 134
GLMC G 041.9910+0.0795	B	19:07:47.1	08:05:31	0.7	-45 – 134
GLMC G 042.0982+0.3515	B	19:07:00.5	08:18:45	0.5	-47 – 132
GLMC G 042.1608+0.6079	A	19:06:12.2	08:29:09	0.4	-57 – 123
GLMC G 042.8347-0.2667	B	19:10:36.0	08:40:51	0.6	-44 – 134
GLMC G 043.1195+0.3682	B	19:08:51.1	09:13:36	0.6	-45 – 134
GLMC G 044.2406+0.3086	A	19:11:10.0	10:11:37	0.7	-44 – 135
GLMC G 045.6999-0.2536	B	19:15:57.0	11:13:32	0.4	-58 – 122
GLMC G 046.4995+0.8093	A	19:13:37.4	12:25:39	0.6	-46 – 133
GLMC G 047.4102+0.1366	B	19:17:48.1	12:55:13	0.6	-45 – 134
GLMC G 048.6717-0.3044	A	19:21:50.2	13:49:39	0.6	-44 – 135
GLMC G 050.0366+0.0714	A	19:23:07.6	15:12:30	0.6	-44 – 135
GLMC G 050.8533+0.3305	A	19:23:46.8	16:03:02	0.6	-44 – 135
GLMC G 052.0790+0.2581	A	19:26:28.4	17:05:43	0.6	-43 – 135
GLMC G 052.5815+0.2014	A	19:27:41.1	17:30:36	0.7	-41 – 138
GLMC G 059.1885+0.1053	B	19:41:44.7	23:14:19	0.7	-40 – 139
GLMC G 059.4914-0.0831	B	19:43:06.8	23:24:29	0.7	-40 – 139
GLMC G 062.8607+0.8219	B	19:47:06.1	26:46:40	0.8	-39 – 140
GLMC G 062.9230-0.5845	B	19:52:39.3	26:07:00	0.7	-39 – 140

Fig. 2. The velocity range reported in Table 2 is slightly larger than reported in previous observations (Caswell et al. 1995b; Phillips et al. 1998), extending to a maximum velocity of  $-42.8 \text{ km s}^{-1}$  (compared to  $-46 \text{ km s}^{-1}$ ).

*G326.66+0.52*: The only previous observations of this source were made by Ellingsen et al. (1996) and Fig. 2 shows

that it has changed dramatically in the decade since then, with a number of new spectral features present and an increase in peak flux density of approximately 100 per cent. The nearby source *G326.64+0.61*, which partially overlaps the velocity range of *G326.66+0.52* has also increased sig-





**Figure 2.** Spectra of the 6.7-GHz methanol maser sources detected in the *GLIMPSE*-based search. The dashed spectra shown for G323.740-0.262 is taken from Ellingsen et al. (2004)

nificantly in peak flux density since the 1994 observations of Ellingsen et al. (1996).

*G328.24-0.55/G328.25-0.53*: This pair of sources is separated by 83 arcsec and was detected in the two largest surveys of southern 6.7-GHz methanol masers (Caswell et al. 1995b; Walsh et al. 1997). It has also been studied at high resolution by Phillips et al. (1998) and Dodson et al. (2004) who found both sites of maser emission to be offset from

nearby radio continuum emission. Somewhat unusually for a moderately strong methanol maser, this source has demonstrated significant variability in the strongest spectral features. Goedhart et al. (2004) monitored this source for 4 years and their observations show that the flux density of the emission at  $-44.7 \text{ km s}^{-1}$  monotonically increased from around 550 Jy in 1999 to 800 Jy in 2003. Figure 2 compares two observations of this source separated by a decade (the

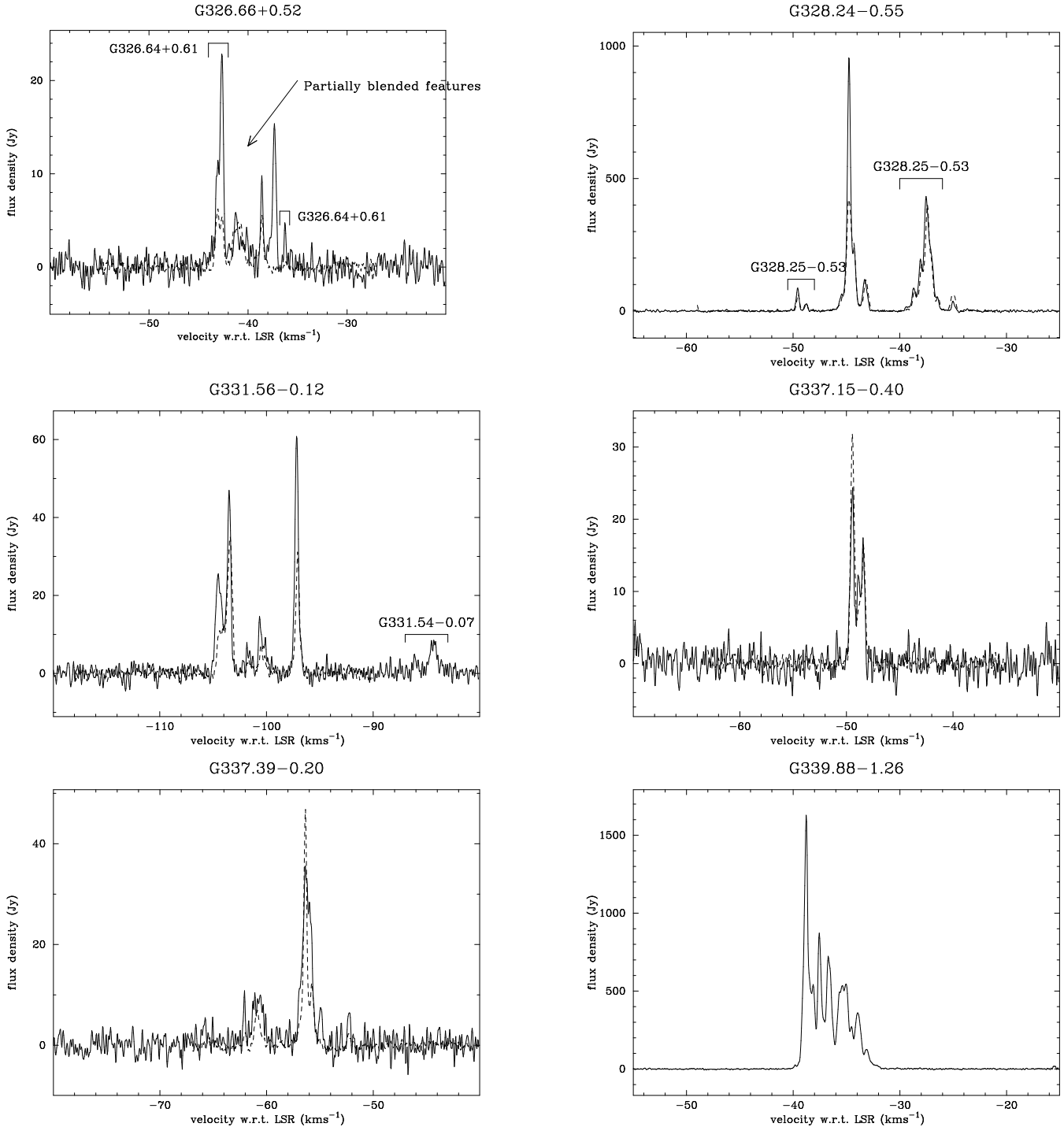


**Figure 2** – *continued* The dashed spectra shown for G326.66+0.52, G328.24-0.55 and G331.56-0.12 are taken from Ellingsen et al. (1996) and those for G337.15-0.40 and G337.39-0.20 are taken from Ellingsen (1996).

spectrum from Ellingsen et al. (1996) uses a dashed line), and shows that the increase in the strongest emission feature has continued and in late 2005 it had a peak flux density of nearly 1000 Jy.

*G331.56-0.12*: This source is listed as not variable by Caswell et al. (1995b), but comparison of the observations in this paper with those of Ellingsen et al. (1996) shows significant variability is present on longer timescales.

*G337.15-0.40*: This source was first detected by Ellingsen (1996), but has not been reported in any refereed publication and so is listed as a new detection here. It's in the Galactic longitude range covered by Caswell (1996), but too far from the Galactic plane to be detected in that search. The overall spectral shape has changed relatively little over the decade between the two observations shown in Fig. 2.

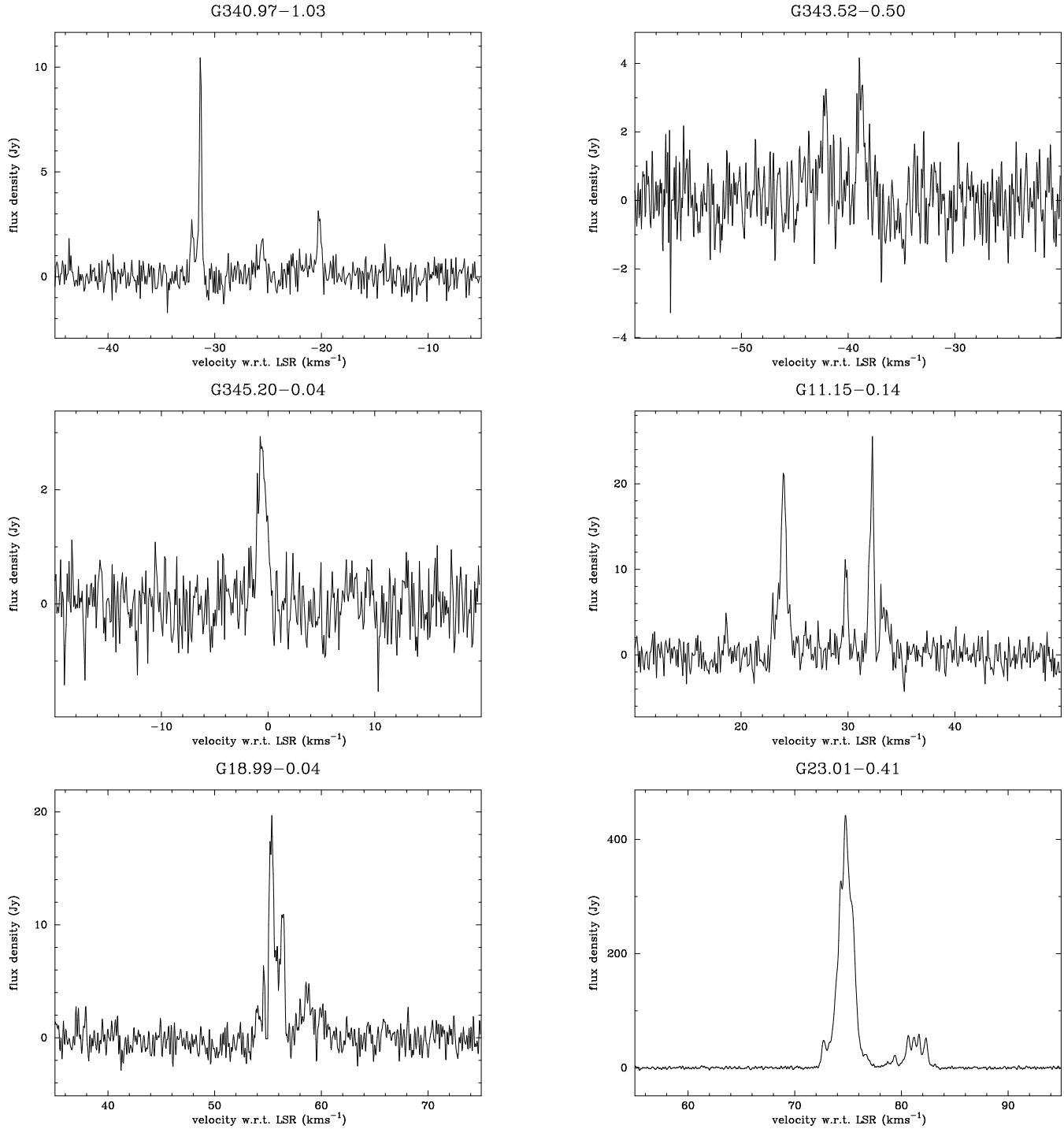


**Figure 2** – *continued* NOTE: The spectrum of G345.20-0.04 was observed at Ceduna and has a velocity resolution of  $0.11 \text{ km s}^{-1}$ , compared to  $0.09 \text{ km s}^{-1}$  for the other spectra.

*G337.39-0.20*: Similar to G337.15-0.40 this source was first detected by Ellingsen (1996), but has not been reported in any refereed publication. The earlier observations show that the velocity range is larger than is apparent from the present epoch and that the peak flux density has decreased by nearly 50 per cent in the decade between 1995 and 2005.

*G339.88-1.26*: This is one of the strongest 6.7-GHz methanol masers known, and it was detected in a distant

sidelobe of an observation of a *GLIMPSE* source more than half a degree away. This source has been the focus of a number of detailed studies as the masers have a linear spatial distribution along the same position angle as extended mid-infrared emission and are projected against a weak ultra-compact HII region (Ellingsen, Norris & McCulloch 1996; Norris et al. 1993; De Buizer et al. 2002). Goedhart et al. (2004) monitored this source for 4 years and found it to

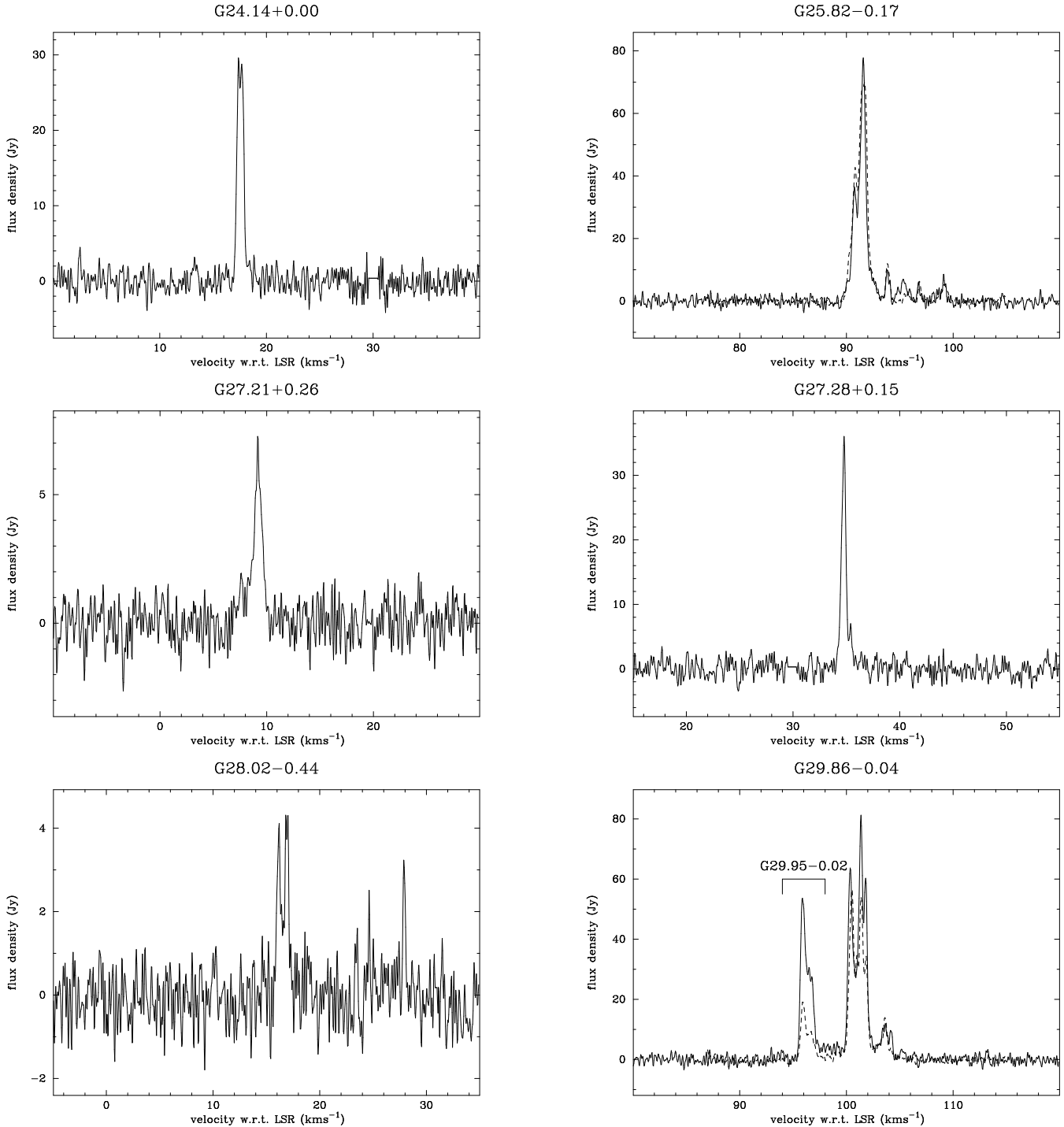


**Figure 2** – *continued* The dashed spectra shown for G25.82-0.17 and G29.86-0.04 are taken from Ellingsen (1996).

show relatively little variation in most spectral features. Figure 2 shows its peak flux density has decreased slightly in comparison to that observed by Caswell et al. (1995b) and Walsh et al. (1997) and several of the weaker features near 30 km s<sup>-1</sup> observed by Caswell et al. (1995b) are no longer detectable.

*G340.97-1.03*: This new detection shows emission over a velocity range of more than 10 km s<sup>-1</sup>, separated into three distinct groups. Most of the spectral features have a flux

density of a few Jy, with the strongest at about 10 Jy. The measured position of the maser is offset by 3.5 arcmin from the *GLIMPSE* source and so the two are very unlikely to be associated.

*G343.52-0.50*: This is one of the weakest 6.7-GHz methanol masers detected in this survey and although the signal to noise ratio of the spectrum shown in Fig. 2 is low it was detected on a total of three separate occasions. The measured position of the maser is 1.7 arcmin from the *GLIMPSE*

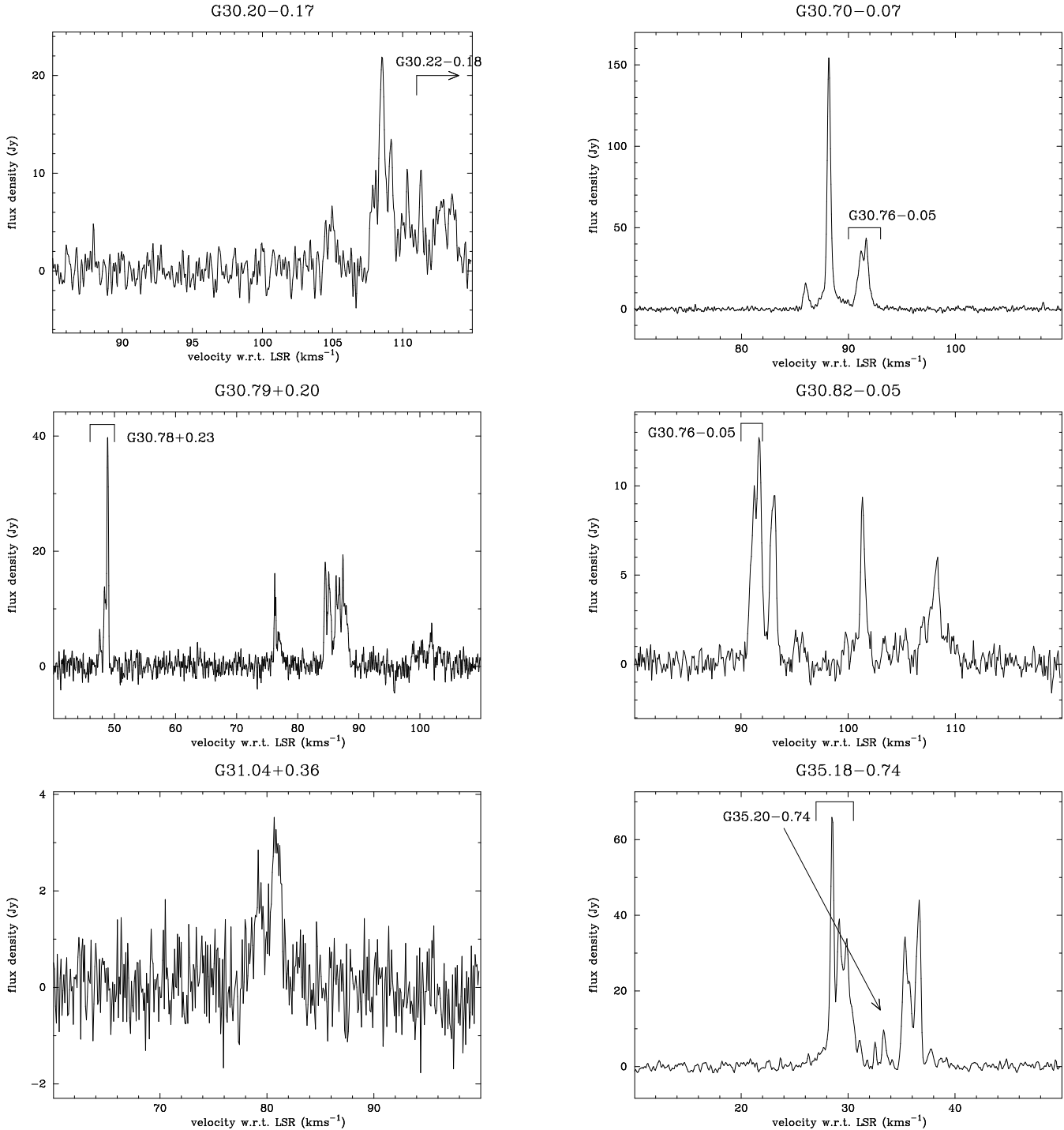


Figure 2 – continued

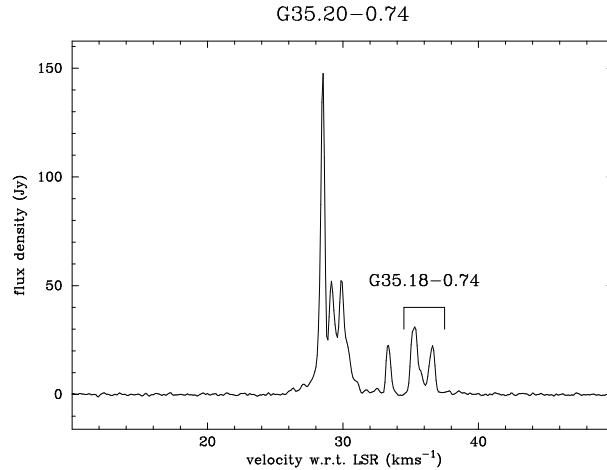
source and so it is possible, but not likely that the two are associated.

*G345.20-0.04*: This is another newly discovered source and is the only one for which the final observation was made at Ceduna rather than Hobart. As a consequence the velocity resolution of the spectrum is  $0.105 \text{ km s}^{-1}$ , compared to  $0.088 \text{ km s}^{-1}$  for the other sources. The measured position of the maser is offset by more than 3.5 arcmin from

the *GLIMPSE* source and so the two are very unlikely to be associated.

*G11.15-0.14*: This moderately strong newly discovered maser has emission covering nearly  $10 \text{ km s}^{-1}$ . As for many of the other new discoveries, the maser emission is significantly offset (6.2 arcmin in this case) from the *GLIMPSE* source towards which the search was made.

*G18.99-0.04*: This newly discovered 6.7-GHz methanol maser is offset by 1.5 arcmin from the *GLIMPSE* source

Figure 2 – *continued*

toward which the search was made, so it is possible, but not likely that the two are associated.

*G23.01-0.41*: The first observation of this strong 6.7-GHz methanol maser was in the 6.7-GHz methanol maser discovery paper of Menten (1991). Caswell et al. (1995b) lists this source as being slightly variable, however, comparison of the spectrum in Fig. 2 with those taken more than a decade earlier shows the peak flux density and overall shape of the spectrum have changed very little, although a weak spectral feature near 70 km s<sup>-1</sup> is no longer present.

*G24.14+0.00*: This source was discovered by Szymczak & Kus (2000) in 1999, and they found it to have a peak flux density of 40 Jy, while the observations of Szymczak et al. (2002) made approximately a year later list a lower value of 26 Jy. Figure 2 shows that 5 years later its peak flux density lies between the two previously reported values and that it continues to show emission over a narrow velocity range.

*G25.82-0.17*: This source was first discovered by Schutte et al. (1993) and has subsequently been detected in a number of *IRAS*-based (Walsh et al. 1997; Szymczak & Kus 2000) and untargeted surveys (Ellingsen 1996; Szymczak et al. 2002). The peak flux density in the spectrum of Schutte et al. (1993) is similar to that seen in Fig. 2 (although it doesn't appear to agree with the value listed in Table 2 of Schutte et al.), while Szymczak et al. (2002) report 66 Jy. The observations of Szymczak & Kus (2000) show a peak flux density of approximately 20 Jy, but it appears that this is largely due to an offset between the maser location and the position of the *IRAS* source targeted. Figure 2 shows the spectrum observed by Ellingsen (1996) as a dashed line, which along with the other observations suggests that the source shows variations of tens of per cent on timescales of years.

*G27.21+0.26*: This source was discovered by Szymczak et al. (2002) and has roughly doubled in peak flux density in the 5 years since their observations.

*G27.28+0.15*: This source was discovered by Slysh et al. (1999) who quote its peak flux density as 41 Jy in 1995, although their spectrum shows approximately 28 Jy. It has also been observed by Szymczak & Kus (2000) and Szymczak et al. (2002) who measured its peak

flux density to be 21 and 23 Jy respectively. Figure 2 shows the current peak flux density to have increased to 36 Jy.

*G28.02-0.44*: This source was discovered by Szymczak et al. (2002) who observed emission of comparable strength over the same, large velocity range as seen in Fig. 2.

*G29.86-0.04*: This source has been previously observed by a number of other authors and shows modest variability. Its peak flux density was 67 Jy in 1992 (Caswell et al. 1995b), 57 Jy in 1995 (Ellingsen 1996), 52 Jy in 2000 (Szymczak et al. 2002), but is currently in excess of 80 Jy. Figure 2 shows the spectrum observed by Ellingsen (1996) as a dashed line and significant variations in the relative intensity are clearly apparent.

*G30.20-0.17*: This source was detected at the edge of the observed velocity range. Comparison of the spectrum in Fig. 2 with that from Caswell et al. (1995b) shows emission previously extended to lower velocities and this may still be present, but beneath the detection threshold of the current observations. The peak and integrated flux densities are comparable to those reported by Szymczak et al. (2002).

*G30.70-0.07*: This source was first observed by Menten (1991), who reported a peak flux density of 125 Jy in 1990. Caswell et al. (1995b) measured a lower peak flux density of 88 Jy two years later and list it as being a slightly variable source. The current observations show a greater peak flux density than any previously reported (154 Jy), although the strength of some of the secondary features has not changed as much.

*G30.79+0.20*: This source was discovered by Caswell et al. (1995b) who found it to exhibit emission in two groups over a velocity range of 75–89 km s<sup>-1</sup>, similar to that observed by Szymczak et al. (2002). Figure 2 shows emission over this range, but also a number of weak features near 100 km s<sup>-1</sup>. Given that emission in this range was not observed on previous occasions, it is probably the nearby source G30.89+0.17 detected in the telescope sidelobes. The peak flux density of the emission near 76 km s<sup>-1</sup> has more than tripled in the period between 1992 and 2005.

*G30.82-0.05*: This source shows emission over an usually large velocity range (nearly 20 km s<sup>-1</sup>). In previous

observations the peak flux density has been observed near  $101 \text{ km s}^{-1}$ , however, this spectral feature has gradually declined in strength over the last 15 years. The strongest spectral feature in the current observations is at a velocity of  $91.7 \text{ km s}^{-1}$ .

*G31.04+0.36*: This source was discovered by Szymczak & Kus (2000) who observed it to have a slightly greater flux density, but the spectrum is overall very similar to that shown in Fig. 2.

*G35.18-0.74*: This source was discovered when making a 5-point grid observation of G35.20-0.74 which showed the highest velocity emission is offset by 1.3 arcmin to the southwest. Comparison of the spectra of G35.18-0.74 and G35.20-0.74 in Fig. 2 shows that their velocity ranges partially overlap, although G35.18-0.74 has a number of spectral features which are not blended, with the strongest emission at velocities greater than  $34 \text{ km s}^{-1}$ . Emission from this source is not evident in the G35.20-0.74 spectrum of Caswell et al. (1995b), but can be seen in the *IRAS*18556+0136 spectrum of Szymczak & Kus (2000), although it was not recognised as a separate source.

*G35.20-0.74/G35.18-0.74*: Caswell et al. (1995b) did not detect any variability in G35.20-0.74 in their 1992/3 observations, however it has increased in peak flux density by approximately 20 per cent over the last 13 years. Emission from G35.20-0.74 extends to about  $35 \text{ km s}^{-1}$ , though this feature overlaps in velocity with the strongest emission in G35.18-0.74.

## 4 DISCUSSION

The primary purpose of the observations presented in this paper was to determine whether, of the *GLIMPSE* sources identified by E06 as being likely to be young high-mass star formation regions with an associated methanol maser, those with the most extreme  $8.0\text{-}\mu\text{m}$  intensity, or reddest [3.6]-[4.5] colours have a greater detection rate than the average. E06 predicted that around 11 per cent of *GLIMPSE* sources meeting the criteria of [8.0] < 10 magnitude and [3.6]-[4.5] > 1.3 should have an associated methanol maser within 3.5 arcmin. A search towards 200 *GLIMPSE* sources meeting these criteria should therefore yield around 22 methanol maser detections within 3.5 arcmin of the infrared source. A total of thirty-eight 6.7-GHz methanol masers were detected in observations towards 27 of the *GLIMPSE* sources, however, only nine of these are new discoveries. For the other nineteen *GLIMPSE* sources where a previously detected 6.7-GHz methanol maser source was observed, in all cases the separation is more than 3.5 arcmin. Of the nine new discoveries, six are within 3.5 arcmin of the *GLIMPSE* source, but only one (G317.47-0.41) is at a separation of less than 1 arcmin. This means that the number of newly detected masers associated with *GLIMPSE* sources is less than 30 per cent of the number predicted (22). These results show that the hypothesis that the most extreme *GLIMPSE* sources meeting the E06 criteria are more likely to have an associated 6.7-GHz methanol maser is incorrect and the reasons why need to be investigated.

The methanol maser selection criteria of E06 only set a lower bound for the [3.6]-[4.5] colour and an upper bound for the  $8.0\text{-}\mu\text{m}$  intensity. It may be the case that the *GLIMPSE*

point sources associated with 6.7-GHz methanol masers are confined to a narrower range of  $8.0\text{-}\mu\text{m}$  intensities and/or [3.6]-[4.5] colours within this box, and lower and upper bounds respectively should be sought. The E06 criteria were determined by examining the *GLIMPSE* point sources associated with a sample of 189 6.7-GHz methanol masers drawn from Caswell (1996), Walsh et al. (1998) and Ellingsen (2005), whose positions are all known to sub-arcsecond accuracy. Of these 189 6.7-GHz methanol masers 82 have a *GLIMPSE* point source within 2 arcseconds. Sixty three of the *GLIMPSE* point sources with an associated methanol maser have an  $8.0\text{-}\mu\text{m}$  intensity measurement and for seven (11 per cent) it is less than 4.58 magnitudes. Fifty three of the *GLIMPSE* point sources have both 3.6- and  $4.5\text{-}\mu\text{m}$  measurements, and of these the [3.6]-[4.5] colour is greater than 2.87 magnitudes for eight (15 per cent). So only a relatively small percentage of currently known 6.7-GHz methanol maser sources match the more extreme criteria used here to select target *GLIMPSE* point sources. However, the more important question is whether this is because only a small number of sources with these criteria are associated with methanol masers, or if it is because there are relatively few sources that meet these criteria. The 2005 April 15 release of the *GLIMPSE* point source catalogue contains 30.2 million sources and of these there are 138 which meet the criteria  $8.0\text{-}\mu\text{m}$  intensity less than 10.0 magnitudes and [3.6]-[4.5] colour > 2.87 magnitudes (category A) and 122 which meet the criteria  $8.0\text{-}\mu\text{m}$  intensity less than 4.58 magnitudes and [3.6]-[4.5] colour > 1.3 magnitudes (category B). A total of 5675 *GLIMPSE* point sources meet the E06 criteria, of which approximately two per cent fall within the category A and category B regions. So approximately a quarter of the 6.7-GHz methanol masers for which a *GLIMPSE* association can reliably determined are associated with sources in either category A or B, which represent less than 5 per cent of the sources meeting the E06 criteria. So the *a priori* evidence was that the most extreme sources meeting the E06 criteria do have a greater than average chance of having an associated 6.7-GHz methanol maser.

If 6.7-GHz methanol masers associated with *GLIMPSE* point sources in category A and/or B typically have a high peak flux density then they would be more likely to have been detected in previous searches. Of the eight known 6.7-GHz methanol masers associated with category A sources, six have a peak flux density greater than 30 Jy. In contrast less than 30 per cent of the 519 sources in the Pestalozzi et al. catalogue of 6.7-GHz methanol masers have a peak flux density greater than 30 Jy. For the seven 6.7-GHz methanol masers associated with a category B source, three have a peak flux density greater than 30 Jy. Given the small number of masers associated with *GLIMPSE* point sources in either category A or B, it isn't possible to draw firm conclusions, but it appears likely that those associated with category A sources often have a higher peak flux density than the majority of 6.7-GHz methanol masers. This does not necessarily imply that these masers are intrinsically more luminous, as selection effects may mean that we don't see extreme [3.6]-[4.5] colours for distant sources in the *GLIMPSE* data.

Another possible reason for the unexpectedly low detection rate for new 6.7-GHz methanol masers could be that many of the *GLIMPSE* sources in category A and B have

previously been observed in either targeted or untargeted searches. A number of regions of the Galactic plane have previously been subjected to untargeted searches (Caswell 1996; Ellingsen et al. 1996; Szymczak et al. 2002). Approximately one quarter of the targeted *GLIMPSE* sources were within these regions. It could be argued that these should have been excluded as part of the selection process, however, they were included to see if they would lead to the discovery of any new sources in the regions. Since interstellar masers are variable it is likely that a single epoch untargeted search will miss some sources which happen to be beneath the detection threshold at the time of the search. The fact that no new masers were found in the regions that had previously been subject to untargeted searches suggests that the number of 6.7-GHz methanol masers missed in untargeted searches due to variability is low. The main targeted searches have been toward previously known main-line OH maser sources and *IRAS* sources meeting the Wood & Churchwell (1989) ultra-compact HII region criteria. The detection rate of 6.7-GHz methanol maser sites towards previously known main-line OH masers resulted in very high detection rates (e.g. Menten 1991; Caswell et al. 1995b), so we need only consider the *IRAS*-based searches here. Of the 200 targeted *GLIMPSE* sources, 77 are within 30 arcseconds of an *IRAS* source. However, only six of these *IRAS* sources meet the Wood & Churchwell criteria of  $\text{Log}_{10}(S_{60}/S_{12}) \geq 1.30$  &  $\text{Log}_{10}(S_{25}/S_{12}) \geq 0.57$ , and of these six none are associated with detected 6.7-GHz methanol masers. This means that few of the *GLIMPSE* source positions targeted here would have been targeted in previous *IRAS*-based searches.

The investigations above demonstrate that the unexpectedly low detection rate of new 6.7-GHz methanol masers is not due to flaws in the selection process for the target sources. The most likely other reasons for the low detection rate are either that the target sources are primarily not regions of high-mass star formation, or that they are regions of high-mass star formation prior to or post the 6.7-GHz methanol maser evolutionary phase. That only six of the 200 target *GLIMPSE* sources are within 30 arcseconds of an *IRAS* source with ultra-compact HII region colours would appear to rule out the possibility that they are post the 6.7-GHz methanol maser evolutionary phase. While the possibility that they are not high-mass star formation regions cannot be ruled out, their extreme mid-infrared colours suggest that many may be very young high-mass star formation regions, prior to the evolutionary phase associated with 6.7-GHz methanol masers.

From the large number of previously known sources detected, it is clear that the estimates of E06 are conservative and that masers separated by more than 3.5 arcmin from the *GLIMPSE* source are frequently detected. This is particularly true for the stronger 6.7-GHz methanol masers which in some cases have been detected when separated by more than 30 arcmin from the *GLIMPSE* source. The results presented in Tables 1 & 2 show that sources with peak flux density less than 10 Jy are detected up to a maximum separation of about 5 arcmin, increasing to about 8 arcmin for a peak flux density less than 100 Jy. The current search excluded from the target list all *GLIMPSE* sources within 3.5 arcmin (half the FWHM of the Mt Pleasant antenna beam at 6.7 GHz) of known methanol maser sources. Given that many methanol maser sources are moderately strong

this exclusion radius should probably be increased by 50 or 100 per cent in future similar searches to reduce the number of redetections of known sources.

#### 4.1 Long-term variability

Table 4 compares the number of spectral features identified in pre-1995 spectra of 6.7-GHz methanol masers taken from the literature (where available) to those in Fig. 2. Determining which spectral features have appeared or disappeared is quite subjective. For example, for sources where there are a large number of spectral features in a relatively small velocity range (e.g. G339.88-1.26 or G23.01-0.41) it is impossible to assess from single dish spectra whether weaker spectral features have appeared or disappeared. In other cases the observations in this paper have a poorer signal to noise ratio than those from Caswell et al. (1995b) and determining whether a spectral feature has disappeared, or is simply too weak to identify in the 2005 spectrum is not possible. Despite these limitations it is possible to use the available spectra to make a crude estimate of the number of spectral features which have appeared and disappeared. The pre-1995 spectra for the 22 sources listed in Table 4 contain 156 identifiable spectral features. Of the 22 sources, 10 showed no change in the number and velocity of spectral features in the 2005 spectra. For the other 12 sources there were either one or two spectral features identified as having either appeared or disappeared. We can obtain a crude estimate of the average lifetime of an individual 6.7-GHz methanol maser spectral feature from the percentage of spectral features that either appear or disappear over the given period. The results summarised in Table 4 suggest that around 6 per cent (taking the mean of the appear and disappear numbers) of 6.7-GHz methanol maser features in a spectrum will change over a ten year period, implying an average lifetime of approximately 150 years. This is very much longer than the typical lifetime of water masers, implying that the environment in which methanol masers arise must be much more stable. It also means that it should be possible to track individual methanol maser features in VLBI proper motion experiments on timescales of decades.

## 5 CONCLUSIONS

The *GLIMPSE* point source catalogue has been used to identify regions likely associated with high-mass star formation at the evolutionary phase when 6.7-GHz methanol masers occur. A search of the 200 most extreme sources meeting the selection criteria of E06 detected only nine new 6.7-GHz methanol masers, significantly less than expected. This implies that the most extreme sources meeting the E06 criteria are less likely than average to have an associated methanol maser, they may be associated with high-mass star formation prior to the 6.7-GHz methanol maser evolutionary phase.

Comparison of the spectra of the previously known 6.7-GHz methanol masers with those observed more than a decade ago (where available) shows that over a ten year period about 6 per cent of the spectral features will disappear and a similar number will appear. This implies the average lifetime of a methanol maser feature is approximately 150



**Table 4.** Comparison of the number of 6.7-GHz methanol maser spectral features observed in 2005 to observations made more than a decade ago. References : a = Caswell et al. (1995b); b = Caswell et al. (1995a); c = Ellingsen et al. (1996); d = Ellingsen (1996).

Methanol maser name	Number of Spectral Features			Reference
	pre-1995	appeared 2005	disappeared 2005	
G 305.20+0.21	3	1	1	a
G 305.21+0.21	7	0	0	a
G 305.25+0.25	2	0	0	a
G 316.81-0.06	7	1	2	b
G 320.23-0.29	11	0	1	b
G 323.46-0.08	2	0	1	a
G 323.74-0.26	15	1	1	a
G 326.66+0.52	2	2	0	c
G 328.24-0.55	10	0	2	a
G 328.25-0.53	9	0	0	a
G 331.56-0.12	7	0	0	a
G 337.15-0.40	3	0	0	d
G 337.39-0.20	6	2	0	d
G 339.88-1.26	15	0	2	a
G 23.01-0.41	14	0	1	a
G 25.82-0.17	7	0	0	d
G 29.86-0.04	7	0	0	a
G 30.20-0.17	6	0	1	a
G 30.70-0.07	4	0	0	a
G 30.79+0.20	8	0	0	a
G 30.82-0.05	11	0	0	a

years, much longer than typically observed for 22-GHz water masers.

## ACKNOWLEDGEMENTS

Financial support for this work was provided by the Australian Research Council. This research has made use of NASA's Astrophysics Data System Abstract Service. This research has made use of data products from the *GLIMPSE* survey, which is a legacy science program of the *Spitzer Space Telescope*, funded by the National Aeronautics and Space Administration.

## REFERENCES

- Benjamin R. A. et al., 2003, *PASP*, 115, 953  
Brand J., Cesaroni R., Comoretto G., Felli M., Palagi F., Palla F., Valdettaro R., 2003, *A&A*, 407, 573  
Breckenridge S. M., Kukolich S. G., 1995, *ApJ*, 438, 504  
Caswell J. L., 1996, *MNRAS*, 279, 79  
Caswell J. L., Vaile R. A., Ellingsen S. P., 1995, *PASA*, 12, 37  
Caswell J. L., Vaile R. A., Ellingsen S. P., Whiteoak J. B., Norris R. P., 1995, *MNRAS*, 272, 96  
De Buizer J. M., Piña R. K., Telesco C. M., 2000, *ApJSS*, 130, 437  
De Buizer J. M., Walsh A. J., Piña R. K., Phillips C. J., Telesco C. M., 2002, *ApJ*, 564, 327  
Dodson R., Ojha R., Ellingsen S. P., 2004, *MNRAS*, 351, 779  
Egan M. P., Price S. D., Kraemer K. E., Mizuno D. R., Carey S. J., Wright C. O., Engelke C.W., Cohen M., Gugliotti G. M., 2003, The Midcourse Space Experiment Point Source Catalog Version 2.3 Explanatory Guide (AFRL-VS-TR-2003-1589). Natl. Tech. Inf. Serv, Springfield, VA.  
Ellingsen S. P., 1996, PhD Thesis, University of Tasmania  
Ellingsen S. P., 2005, *MNRAS*, 359, 1498  
Ellingsen S. P., 2006, *ApJ*, 638, 241 (E06)  
Ellingsen S. P., Norris R. P., McCulloch P. M., 1996, *MNRAS*, 279, 101  
Ellingsen S. P., von Bibra M. L., McCulloch P. M., Norris R. P., Deshpande A. A., Phillips C. J., 1996, *MNRAS*, 280, 378  
Ellingsen S. P., Cragg D. M., Lovell J. E. J., Sobolev A. M., Ramsdale P. D., Godfrey P. D., 2004, *MNRAS*, 354, 401  
Goedhart S., Gaylard M. J., van der Walt D. J., 2004, *MNRAS*, 355, 553  
MacLeod G. C., Gaylard M. J., 1992, *MNRAS*, 256, 519  
MacLeod G. C., Gaylard M. J., Nicolson G. D., 1992, *MNRAS*, 254, 1P  
Menten K. M., 1991, *ApJ*, 380, L75  
Minier, V., Ellingsen, S. P., Norris, R. P., Booth, R. S., 2003, *A&A*, 403, 1095  
Minier, V., Burton, M. G., Hill, T., Pestalozzi, M. R., Purcell, C. R., Garay, G., Walsh, A. J., Longmore, S., 2005, *A&A*, 429, 945  
Norris R. P., Whiteoak J. B., Caswell J. L., Wieringa M. H., Gough R. G., 1993, *ApJ*, 412, 222  
Pestalozzi, M., Minier, V., Booth, R., 2005, *A&A*, 432, 737  
Phillips C. J., Norris R. P., Ellingsen S. P., McCulloch P. M., 1998, *MNRAS*, 300, 1131  
Schutte A. J., van der Walt D. J., Gaylard M. J., MacLeod G. C., 1993, 261, 783

- Slysh V. I., Val'tts I. E., Kalenskii S. V., Voronkov M. A., Palagi F., Tofani G., Catarzi M., 1999, *A&AS*, 134, 115  
Szymczak M., Kus A. J., 2000, *A&A*, 360, 311  
Szymczak M., Kus A. J., Hrynek G., Kepa, A., Pazderski, E., 2002, *A&A*, 392, 277  
van der Walt J., 2005, *MNRAS*, 360, 153  
van der Walt D. J., Gaylard M. J., MacLeod G. C., 1995, *A&ASS*, 110, 81  
Walsh A. J., Burton M. G., 2006, *MNRAS*, 365, 321  
Walsh A. J., Hyland A. R., Robinson G., Burton M. G., 1997, *MNRAS*, 291, 261  
Walsh A. J., Burton M. G., Hyland A. R., Robinson G., 1998, *MNRAS*, 301, 640  
Walsh A. J., Bertoldi F., Burton M. G., Nikola T., 2001, *MNRAS*, 326, 36  
Walsh A. J., Lee J.-K., Burton M. G., 2002, *MNRAS*, 329, 475  
Wood D. O. S., Churchwell E., 1989, *ApJ*, 340, 265